

“Thermal Properties of Fe₂O₃ Magnetic Nano-Particles as a Function of Concentration under Low Frequency Magnetic Field”

E. I. A. Elbeshir

Al Baha University, Faculty of Science and Art, Almakhwah, Physics Department, P.O.

Box.1988 AL Baha, KSA

Alneelain University, Faculty of Science and Technology, Department of Physics and Applied

Physics, Khartoum, SUD

abugomry@yahoo.com

Abstract

A powder sample of Fe₂O₃ magnetic nanoparticles (MNPs) has been synthesized by co-precipitation method, Transmission Electron Microscope (TEM) and X-Ray Diffraction (XRD) were used to the characterize the sample size and the average size is reported (t = 44 nm).

Different suspensions (S₁, S₅, S₁₀, S₁₅ and S₂₀) were made by adding different concentrations (X = 1, 5, 10, 15 and 20 mg of the Fe₂O₃ MNPs) to 1mL of distil water (DW) respectively. An induction heater operated at low frequencies was used to study the thermal properties of these suspensions. The results showed that: the maximum temperature T_{max} = (50, 49, 46, 45 and 42 °C), the heating rate $\Delta T/\Delta t = (28.3 \times 10^{-3}, 26.7 \times 10^{-3}, 25.0 \times 10^{-3}, 23.3 \times 10^{-3}$ and $18.3 \times 10^{-3} \text{ } ^\circ\text{C/s}$) and the specific absorption rate SAR = (118.4, 22.4, 10.5, 6.5 and 3.8 W/ g) respectively for the suspensions (S₁, S₅, S₁₀, S₁₅ and S₂₀).

Keywords: Fe₂O₃ nanoparticles, SAR, thermal properties, hyperthermia.

المخلص:

تم تصنيع عينة مسحوق من الجسيمات النانوية المغناطيسية Fe₂O₃ (MNPs) بطريقة الترسيب المشترك، وتم استخدام مجهر الإرسال الإلكتروني TEM وانحراف الأشعة السينية (XRD) لتوصيف حجم العينة وتم الإبلاغ عن متوسط الحجم (t=44) نانومتر.

تم عمل معلقات مختلفة (S₁, S₅, S₁₀, S₁₅ and S₂₀) بإضافة تركيزات مختلفة (X = 1, 5, 10, 15 and 20 mg of the Fe₂O₃ MNPs) إلى 1 مل من ماء التقطير (DW) على التوالي. تم استخدام سخان حثي يعمل على ترددات منخفضة لدراسة الخصائص الحرارية لهذه المعلقات. أظهرت النتائج أن: درجة الحرارة القصوى (50, 49, 46, 45 and 42 °C)، معدل التسخين $\Delta T/\Delta t = (28.3 \times 10^{-3}, 26.7 \times 10^{-3}, 25.0 \times 10^{-3}, 23.3 \times 10^{-3}$ and $18.3 \times 10^{-3} \text{ } ^\circ\text{C/s}$) ومعدل الامتصاص النوعي SAR = (118.4, 22.4, 10.5, 6.5 and 3.8 W/ g) على التوالي للتعليق (S₁, S₅, S₁₀, S₁₅ and S₂₀).

الكلمات المفتاحية: جزيئات Fe₂O₃ النانوية، SAR، الخواص الحرارية، ارتفاع الحرارة.

1. Introduction.

Maghemite ($\text{-Fe}_2\text{O}_3$) and other magnetic nanoparticles (MNPs) have great promise as nanomaterials for use in fields as diverse as photo catalysis, photonics, magnetic storage, electronics, medicine, and theranostics. Excellent and distinctive magneto-thermal qualities make them useful in a variety of applications, including magnetic resonance imaging, magnetic drug targeting, and magnetic fluid hyperthermia. As a noninvasive cancer treatment, magnetic hyperthermia makes use of the heat generated by MNPs in an alternating magnetic field (AMF) to remove sick tumour areas and kill cancerous cells. The specific absorption rate (SAR), the amount of heat produced per unit time and per unit gramme of the magnetic material, is commonly used to characterize the heat created by MNPs in the presence of AMF. To improve the heating powers of magnetic hyperthermia treatments, various research groups, including ourselves, have synthesized $\text{-Fe}_2\text{O}_3$ NPs using different ways and explored the impact of many parameters on the SAR values. Previous research showed that adjusting the saturation magnetization, size, NP concentration, preparation procedure, and amplitude and frequency of the applied magnetic field can all affect the SAR readings [1]. For instance, for 12 nm $\text{-Fe}_2\text{O}_3$ NPs produced using the co-precipitation method, De la Presa et al. found a SAR value of 58 W/g. With the sol-gel approach, our team was able to synthesis 14 nm $\text{-Fe}_2\text{O}_3$ NPs with a SAR value of 30 W/g. In particular, doping the nanostructures of $\text{-Fe}_2\text{O}_3$ with alkaline earth and transition metals can be used to fine-tune the material's heating efficiency. Saturation, Curie temperature, and the heating of MNPs could all be adjusted in this way. Doping $\text{-Fe}_2\text{O}_3$ NPs with Gadolinium (Gd) has recently caught our attention as a potential way to increase their heating capacity. We found that Gd-doped $\text{-Fe}_2\text{O}_3$ showed great heating efficiencies (120 W/g) and attained magnetic hyperthermia temperatures (42 °C) in relatively short timeframes despite the loss of magnetic saturation (6 min). To further reduce heating potentials, we also synthesized $\text{-Fe}_2\text{O}_3\text{-TiO}_2$ nanocomposites with SAR values = 40 W/g, which were found to be lower than undoped $\text{-Fe}_2\text{O}_3$ (SAR 90 W/g) [2,3].

It has been known for quite some time that one can make advantage of the heat that is produced by magnetic nanoparticles (MNPs) when they are subjected to an external alternative magnetic field (EAMF). This generated heat, which is based on the Neil-Brown relaxation time, is dependent on a number of elements, some of which are the frequency and intensity of the applied EAMF, as well as the size and concentration of the sample itself [4-7].

The relationship between the thermal characteristics of MNPs and the frequencies, intensities, and strengths of magnetic fields was one of the topics that the researchers were looking at. Research should also be done on the influence that high frequency has on the size, coating, and concentration of MNPs [8,9].

It is common knowledge that there is a one-to-one correlation between the magnitude of the magnetic field that is imposed on an MNP and the amount of heat that is produced by the MNP. When it came to therapeutic applications, the high external magnetic field that was applied to the sample was more detrimental than helpful since it affected healthy cells. Recent research has shown that the desired results can be obtained from the thermal characteristics of MNPs at the lowest feasible frequency of the magnetic field that is applied to them. In the course of this investigation, an external magnetic field with a frequency of one hundred kilohertz has been utilised in order to investigate the impact that the concentration of a sample of Fe_2O_3 has on its thermal properties.

In this research, we will investigate the relationship between the concentration of the Fe₂O₃ MNPs /ml and the thermal properties of the sample, such as the maximum temperature T max in o C, the heating rate T/t in o C/s and the specific absorption rate SAR in W/g. This will be done after preparing different suspensions (S1, S5, S10, S15 and S20) respectively for the concentrations (X= 1, 5, 10, 15, and 20 mg.

1.1. Study problem:

The problem of this study is that despite the many benefits of using magnetic nanoparticles, there are side effects of using magnetic nanoparticles Fe₂O₃ and attention must be drawn to them and taken into account so that they can be easily avoided. These relics are further researched.

1.2. the importance of studying:

The importance of this study is that it works to clarify the relationship between the concentration of Fe₂O₃ MNPs / ml and the thermal properties of the sample such as the maximum temperature T max in o C, the heating rate $\Delta T / t$ in oC / s and the specific absorption rate SAR in W / g after preparation different suspensions (S1, S5, S10, S15, and S20) respectively for concentrations (X = 1, 5, 10, 15, and 20 mg of Fe₂O₃ MNPs + 1 ml of distal water DW).

1.3. Objectives of the study:

This study aims to determine and know the thermal properties of Fe₂O₃ magnetic nanoparticles as a function of concentration under low-frequency magnetic field.

Theoretical framework and previous studies

2. Synthesis of Magnetic Nanoparticles.

There are three main approaches to NP synthesis: chemical, physical, and biological. Due to the vast number of NP synthesis methods ranging from precipitation to sophisticated procedures and complex, the chemical and physical classifications are the most commonly utilized. Micro emulsions, hydrothermal reactions, hydrolysis, sonolysis, hemolysis, electrochemistry, flow injection, electrospray, reduction, micellar, and gamma rays are just a few of the most common synthesis methods; each of these methods is carried out under different synthesis conditions that alter the physicochemical properties of MNPs, and thus produce different magnetic properties [10].

MNPs of varying compositions, such as Fe₃O₄ and -Fe₂O₃, as well as other NPs using a single element in their composition, such as Fe, Co, and Ni, are commonly obtained using precipitation and precipitation processes. Nonetheless, the chemical makeup of various MNPs with medicinal uses varies widely, ranging from metal and alloys like Fe-Pd and Mn-Zn-Gd-ferrite to lanthanides like Ln(III): Fe₃O₄ and other compounds (Sm, Eu, Gd). Furthermore, this technology has enabled the manufacture of bioactive ferromagnetic glass-ceramic MNPs coated in apatite analogous to bone, which binds proteins and medicines while maintaining proper orientation to the damaged tissue [11].

2.1. Synthesis of Magnetic Nanoparticles.

It is common practise to synthesize magnetic nanoparticles (MNPs) with magnetic metal oxide nuclei by precipitation or precipitation from the corresponding salts in a basic medium, inert atmosphere, and at room temperature or higher. Once the reaction conditions are optimized, the method is highly reproducible, allowing for the size dispersion to be decreased. The most common MNPs synthesized using this technique are Fe₃O₄ or -Fe₂O₃ NPs, both of which are derived from Fe²⁺/Fe³⁺. The reaction medium's temperature, pH, and ionic strength are all crucial components in the synthesis of these MNPs. Low environmental stability was demonstrated by these MNPs, which were either oxidized or dissolved in an acid media. By exposing Fe₃O₄ or -Fe₂O₃ MNPs to a Fe³⁺ solution during production, the particles are oxidized and become stable in both acidic and basic environments.

Although it is difficult to promote homogeneous nucleation of MNPs, the true problem lies in regulating particle size to achieve a narrow size distribution during a sluggish nucleus growth. This type of synthesis typically results in fairly polydisperse NPs, and temperature is one of the most critical parameters controlling nucleus growth. If the synthesis conditions can be standardized and controlled well enough, however, NPs with low disparity can be obtained [12].

In addition to their primary purpose of stabilizing the NPs produced through precipitation and precipitation processes, the additives can also serve as a reducing agent, facilitating nucleation. Polyvinyl alcohol (PVA), poloxamers, polo amines, oleic acid, derivatives of poly (ethylene glycol) (PEG), and even liposomes are all substances employed as stabilizing or reducing agents. Case in point: the

In the synthesis of MNPs, the concentrations of PVA and citric acid can be adjusted to change the NPs' size and shape. However, chelation of metal ions can influence nucleation, causing larger particles to form due to the poor availability of nuclei in the reaction system and leading to a tremendous growth of the available nuclei, with the particle growth dominating the synthesis system. Adsorption of chemicals on the nuclei as coatings can also slow growth, which is conducive to the creation of smaller NPs [13].

2.2. Thermal Decomposition.

By heating organometallic compounds in organic solvents (with a high boiling point) and stabilizing agents, NPs can be synthesized (i.e., surfactants). Synthesized with acetylketonates, N-nitrosophenylhydroxylamine (cup-ferronates), carbonyls, and other organometallic precursors with metallic cores are NPs. Some examples include the use of stabilizing agents such as Fe^{2+,3+}, Mn^{2+,3+}, Co^{2+,3+}, and Ni^{2+,3+}, as well as fatty acids, oleic acids, and hexadecylamine. The organometallic compound's zero-oxidation-state metallic centres (i.e., Fe(CO)₅) determine the sort of NPs that can be generated. In contrast, the usage of [Fe(acac)₃] as a precursor results in the formation of metal oxide NPs, such as Fe₃O₄. Additional NPs with magnetic alloys like CoPt₃ and FePt can be created by combining metal precursors in the reaction system. These MNPs display enormous coercivities, strong anisotropy, and high magnetic susceptibility [14].

The reaction rate, morphology, and size of the NPs are all modifiable by adjusting the reagent ratios, which are determined by the source of metal ions, stabilizing agent, solvent, reaction time, and temperature, respectively. The

stabilizer's design is another factor to think about. For instance, when using fatty acids as stabilisers, the reaction rate can be altered by adjusting the chain length of the fatty acids' alkyl chain. Jana et al. utilized these factors when they created metal oxide MNPs with tunable size and shape by concentration and reactivity. These MNPs included Fe₃O₄, Cr₂O₃, MnO, Co₃O₄, and NiO. Example: by extending the reaction time, virtually monodispersed NPs in the range of 6-50 nm in size and various forms (including points and cubes) were generated from iron oxide using metal fatty acid salts [15].

A simple synthesis employing FeCl₃ 6H₂O as the iron source and 2-pyrrolidone as the coordination solvent was also used to produce water-soluble magnetite NPs. The reaction period determined the NPs' final sizes; at 1, 10, and 24 hours, the smallest NPs measured 4 nm and the largest 60 nm. The morphology of the NPs was likewise altered by the reaction period, going from spherical at the beginning to cubic at the end. Recently, the same team used the same reaction conditions to create water-soluble MNPs by adding a dicarboxylic-terminated PEG as a surface-protecting agent. Magnetic resonance imaging (MRI) contrast agents using MNPs showed promise for detecting malignant tissue.

Nanoparticles (NPs) can be obtained from suitable metal carbonyl sources, but metal oxide synthesis is still the most common method. The increased magnetization of metallic NPs compared to the NPs of their respective oxides makes them of interest not only in the medical but also the industrial sphere, particularly in data storage [16]. For instance, Fe MNPs were synthesized by adding polyisobutene to decalin with an iron source of Fe(CO)₅ at 170 degrees Celsius in an inert nitrogen environment, yielding a particle size range of 2-10 nm and a polydispersity of 10% depending on the Fe(CO)₅/polyisobutene ratio. Cobalt MNPs were synthesized by reacting [Co₂(CO)₈] with aluminum alkyl compounds (AlR₃), with the particle size of the Co MNPs varying from 3 to 11 nm depending on the length of the alkyl (R) chain utilized in the synthesis. Strong oxidation under air environment was also seen, therefore these particles would need to be treated afterward.

treated with polymer coatings to prevent oxidation, resulting in MNPs that are stable in air and hence preferable for use in oxidizing environments because of their portability and relative simplicity to handle, store, and apply [17].

2.3. Micro emulsion.

Droplets between 1 and 50 nm in size are formed when an immiscible liquid is dispersed in a miscible liquid (often water), and these droplets are stabilized by the presence of a surfactant. Since micro emulsions can create micro droplets containing the necessary reagents, they can be employed as a nonreactor capable of producing NPs. To complete the NP production process, the droplets collide and merge in the reaction system, combining the chemicals. Polydispersity, low yield of NPs, huge quantities of solvents required, and poor variety in metal precursors are some of the disadvantages of this approach when compared to precipitation and thermal decomposition synthesis. Therefore, synthesis of NPs via micro emulsion would be a challenging process [18].

Despite the disadvantages of the micro emulsion process, a wide variety of NPs have been synthesized, such as Fe₃O₄ NPs or MFe₂O₄ alloys with Co, Cu, Ni, Cd, etc., altering their magnetic characteristics. One study indicated that the size of MnFe₂O₄-type alloyed NPs generated by reverse micelles employing sodium dodecylbenzenesulfonate as a

surfactant was proportional to the amount of water to solvent used. Sol-gel synthesis employing reverse micelles with $\text{FeCl}_3 \cdot 6\text{H}_2\text{O}$ as the metal source yielded Fe_3O_4 nanorods. Research conducted during synthesis demonstrated that variables such as reaction temperature, environment, and gel hydration level can be used to manipulate the nanorods' phase. However, MNPs alloyed with CoFe_2O_4 were produced by combining FeCl_3 and $\text{Co}(\text{AcO})_2$ in the presence of sodium dodecyl sulphate. The concentrations of the metal sources and the surfactant determined the size of the MNPs. The MNPs had a polydispersity of 30–35%, with an average size range of 2–5 nm [19].

3. Previous studies.

- **Study of (Flores-Rojas, G. G., et al. (2022). Magnetic Nanoparticles for Medical Applications. [20]**

Because they are amenable to modification in accordance with biomedical techniques and guidance by an external magnetic field inside the human body, magnetic nanoparticles (MNPs) are a cutting-edge instrument in the medical profession. The primary goal of this paper is to provide examples of some of the more promising medical applications, such as improved MRI diagnostics, radiation for cancer, improved smart drug delivery systems, and tissue engineering. The second goal is complementary and consists of illuminating the theoretical underpinnings and mechanisms of action associated with magneto responsive materials.

- **Study of (Aldaoud, A., et al. (2022). Magneto-thermal properties of Co-doped maghemite ($\gamma\text{-Fe}_2\text{O}_3$) nanoparticles for magnetic hyperthermia applications. [21]**

In this work, we present the fabrication, characterization, and heating efficiency of both undoped and Cobalt (Co)-doped maghemite ($\gamma\text{-Fe}_2\text{O}_3$) nanoparticles (NPs) for use in magnetic hyperthermia. As-synthesized NPs were completely described with regards to their structure, magnetic characteristics, and heating capacity. XRD and Rietveld investigation demonstrated the production of single cubic phase of $\gamma\text{-Fe}_2\text{O}_3$, where doping with Co did not modify either the crystal structure or the lattice parameter. It was found that Fe ions are tetrahedrally and octahedrally coupled to oxygens and that Co ions occupy the octahedral sites in Co-doped samples. Magnetic measurements indicated growth of magnetic saturation (M_s) with increasing Co concentrations from 0 to 5% (53.14–67.49 emu/g), with negligible coercive field and remanence suggesting superparamagnetic activity. Langevin model and the low of approach to saturation (LAS) were used to confirm superparamagnetism and to establish the effective anisotropy constant (K_{eff}), respectively. The results of the AMF temperature rise tests showed that all the samples have excellent heating efficiency and can achieve hyperthermia temperatures (42 °C) in a short amount of time (3–10 min). Intriguingly, it took $\gamma\text{-Fe}_2\text{O}_3$ NPs only 4 minutes to heat up to 42 °C, but it took 7-10 minutes for $\gamma\text{-Fe}_2\text{O}_3$ NPs doped with 1-5% Co. Surprisingly, SAR (122 W/g) and ILP (1.5 nHm²/kg) values of $\gamma\text{-Fe}_2\text{O}_3$ NPs were found to be greater compared to Co-doped $\gamma\text{-Fe}_2\text{O}_3$ counterparts, showing better heating efficiency of $\gamma\text{-Fe}_2\text{O}_3$ NPs. The mechanism of heating and plausible explanation for this observation is examined. In spite of this, the ILP values for both $\gamma\text{-Fe}_2\text{O}_3$ and 1-5% Co-doped $\gamma\text{-Fe}_2\text{O}_3$ NPs (0.52-1.5 nHm²/kg) are in the range reported for commercial ferrofluids, demonstrating their good heating efficiency and making them viable candidates for magnetic hyperthermia applications.

- **Study of (Rajan, A., Sharma, M., & Sahu, N. K. (2020). Assessing magnetic and inductive thermal properties of various surfactants functionalised Fe₃O₄ nanoparticles for hyperthermia. [22]**

Magnetization measurements have been used to delve into the magnetic characteristics of Fe₂O₃ nanoparticles (average diameter 143 nm) in alumina (68% Fe₂O₃ by weight). The susceptibility displays a maximum at 145 K when cooled to zero fields, and the data point to a superparamagnetic behavior of interacting particles with a distribution of relaxation times as the temperature decreases. As the temperature drops below 60 K, the antiparticle interactions and local surface anisotropy increase, resulting in a new magnetic domain.

- **Study of (Zysler, R. D., Fiorani, D., & Testa, A. M. (2001). Investigation of magnetic properties of interacting Fe₂O₃ nanoparticles. [23]**

However, iron oxides like magnetite (Fe₃O₄) and maghemite are the only ones that can be used in magnetic nanoparticles for magnetic hyperthermia therapy due to biocompatibility concerns (g-Fe₂O₃). The magnetic iron oxide phase 3-Fe₂O₃ possesses remarkable magnetic properties, although it has been overlooked thus far. The magnetic coercivity of 3-Fe₂O₃ is enormous, but that of Fe₃O₄ and g-Fe₂O₃ is quite low. This study investigated the heating power of untreated and polymer-coated samples of 3-Fe₂O₃ and g-Fe₂O₃ nanoparticles over a wide range of field frequencies and amplitudes. It has been discovered that 3-Fe₂O₃ nanoparticles generate the majority of their thermal energy in the low-frequency zone (20-100 kHz) in media with a viscosity close to that of cell cytoplasm. In contrast, high frequency heating is enhanced for g-Fe₂O₃ nanoparticles (400–900 kHz). A significant rate of internalization was seen in cell culture studies, and no toxicity was observed across a broad concentration range of nanoparticles. In conclusion, g-Fe₂O₃ nanoparticles perform better than 3-Fe₂O₃ nanoparticles when used for human magnetic hyperthermia. However, the unique frequency response of these 3-Fe₂O₃ nanoparticles paves the path for reversible magnetic heating.

- **Study of (Elbeshir, E. I. A. (2021). On the gum arabic to improve the thermal properties of Fe₃O₄ nanoparticles. [24]**

This research presents the results of a thermal analysis of a powder sample of Fe₃O₄ magnetic nanoparticles that were generated by the co-precipitation process and characterized via x-ray diffraction and transmission electron microscopy. The thermal characteristics of a sample coated with several concentrations of gum arabic (GA) were measured using an induction heater (X = 0 mg/ml, 20 mg/ml, 40 mg/ml, 60 mg/ml, and 80 mg/ml). It was found that the thermal characteristics of the sample changed with increasing levels of GA. The specific heat capacity (CG) of the GA solution was also observed to decrease as its concentration was raised.

- **Study of (Soares, P. I., et al. (2015). Thermal and magnetic properties of iron oxide colloids: influence of surfactants. [25]**

Multiple biomedical applications, including MRI, drug delivery, and hyperthermia, have piqued researchers' interest in iron oxide nanoparticles (NPs) over the past few decades. With the use of magnetic NPs and an external magnetic field, a therapy method known as hyperthermia can raise the temperature of cancer cells to between 41 and 45 degrees Celsius, killing the cells. Iron oxide nanoparticles (NPs) coated with oleic acid and trisodium citrate were synthesised

via chemical precipitation and measured to have a size of 9 nm. Both stabilisers were tested to see how they affected the resulting iron oxide NPs' heating capacity and in vitro cytotoxicity. Physical and chemical analysis of the samples showed that the presence of the surfactants strongly affected both the magnetic characteristics and the heating ability, but did not alter the average particle size. The heating ability of Fe₃O₄ NPs increases as the iron content does, but it diminishes when the NPs are coated with trisodium citrate or oleic acid. According to the results of cytotoxicity tests, neither pure nor trisodium citrate-treated Fe₃O₄ samples were cytotoxic. Cell viability is significantly decreased by oleic acid Fe₃O₄, especially in the SaOs-2 cell line. The manufactured iron oxide NPs are well-suited for hyperthermia treatment of cancer, and the addition of a surfactant provides significant benefits in terms of NP dispersion, while also allowing for improved hyperthermia temperature regulation.

- **Study of (Rytov, R. A., Bautin, V. A., & Usov, N. A. (2022). Towards optimal thermal distribution in magnetic hyperthermia. [26]**

It is demonstrated that in magnetic hyperthermia, the best stationary thermal distribution may be achieved using a linear combination of spherically symmetric heat sources. Moreover, for assemblies of magnetic nanoparticles with a modest value of specific absorption rate (SAR), on the range of 100-150W/g, such spatial positioning of heat sources produces acceptable temperature distribution in biological medium. We also show that assemblies of spherical magnetic nanocapsules, which are made of metallic iron nanoparticles encased in nonmagnetic shells of sufficient thickness, can be used effectively to induce magnetic hyperthermia. To lessen the impact of the strong magneto-dipole interaction between closely spaced nanoparticles, we use numerical simulation to optimize the size and geometric structure of biocompatible spherical capsules. At low amplitudes $H_0 = 50-100$ Oe and moderate frequencies $f = 100-200$ kHz of alternating magnetic field, it is shown that capsule assembly may generate sufficient high SAR values of the order of 250-400 W/g, which is suitable for use in clinics.

- **Study of (Ashjaee, M., Afgh, S. S. S., & Karimi, A. (2014). Experimental investigation on thermal conductivity of MFe₂O₄ (M= Fe and Co) magnetic nanofluids under influence of magnetic field. [27]**

Here, we examine the effects of a uniform magnetic field on the thermal conductivity of magnetic nanofluids (MNFs) made up of MFe₂O₄ (M=Fe and Co) nanoparticles suspended in deionized water. Together, Fe₃O₄ and CoFe₂O₄ nanoparticles are generated by the co-precipitation technique. Nanoparticles' structure, size, and magnetic characteristics can be characterized with the help of X-ray diffraction, transmission electronic microscopy, and a vibration sample magnetometer. The thermal conductivity of MNFs is investigated over a wide range of magnetic field strengths (from 0 to 500G) and volume fractions (from 0 to 4.8%). The experimental results reveal that as the volume fraction and magnetic field strength are increased, the thermal conductivity of MNFs increases until it reaches a saturation point. Finally, based on the experimental results, new correlations are offered for predicting the thermal conductivity of MNFs in the absence and presence of a magnetic field.

- **Study of (Shylaja, A., Manikandan, S., Suganthi, K. S., & Rajan, K. S. (2015). Preparation and thermo-physical properties of Fe₂O₃-propylene glycol nanofluids. [28]**

Nanoparticles of iron oxide (Fe₂O₃) were synthesised by reacting ferric chloride and ferrous sulphate in a precipitation apparatus. Using stirred bead milling, shear homogenization, and probe ultra-sonication, Fe₂O₃ nanoparticles were dispersed in propylene glycol to create a nanofluid. Nanofluid properties such as viscosity, particle size distribution, and thermal conductivity were evaluated. At room temperature, the concentration of Fe₂O₃ nanoparticles (0-2 vol%) causes a decrease in viscosity due to interactions between the nanoparticles and propylene glycol on the nanoparticle surfaces. Liquid layering is the primary contribution to the thermal conductivity boost seen for 2 vol% nanofluid at room temperature (21% improvement).

- **Study of (Lukawska, A. B. (2014). Thermal Properties of Magnetic Nanoparticles in External Ac Magnetic Field. [29]**

In this work, we investigate the effect of an external ac magnetic field on the thermal characteristics of magnetic nanoparticles. Thermal breakdown of iron pent carbonyl (Fe(CO)₅) and dicobalt octacarbonyl (Co₂(CO)₈), triscobalt nona(carbonyl)chloride (Co₃(CO)₉Cl), or tetracobalt dodecacarbonyl (Co₄(CO)₁₂) yielded iron and cobalt nanoparticles that were then dried. The average sizes of the samples varied, from 5.6 to 21.4 nm for iron and 6.5 to 19.4 nm for cobalt, respectively. Each sample's temperature rises after being subjected to an alternating magnetic field was recorded. The critical diameters for the transitions from the multi-domain to the single-domain and from the single-domain to the superparamagnetic regime were determined by analyzing the results. Potential uses of the nanoparticles in hyperthermia for cancer treatment were investigated. Given this use, and in an effort to learn more about the effects magnetic nanoparticles would have on human tissue, a Matlab-based mathematical model built on bio-heat equations was presented.

- **Study of (Zouli, N., Mohammed, S. A. M., & Al-Dahhan, M. H. (2017). Enhancement of Heat Transfer Coefficient using Fe₂O₃-Water Nanofluids. [30]**

To investigate the impact of nanofluids with varying concentrations and sizes of nanoparticles on the local heat transfer coefficient, we created a local heat transfer probe that can detect the heat transfer coefficient in a constructed independent effect experimental setting. The nanofluids employed in the experiment were water containing iron (III) oxide (Fe₂O₃) nanoparticles. The Fe₂O₃ nanoparticle diameters ranged from 20 nm to 40 nm. Varying nanoparticle sizes were present at quantities between 0% and 0.09% by volume. The results demonstrate that 0.09% volume concentration of aqueous Fe₂O₃ nanoparticles may greatly boost the heat transfer coefficient in the turbulent flow regime, with the enhancement increasing with Reynolds and Nusselt number, as well as particle concentration. Thermal conductivity was determined and compared to Maxwell's classical model.

4. Experimental.

Co-precipitation was the approach that was utilised in the production of the powder sample of Fe₂O₃ magnetic nanoparticles (MNPs). In this investigation, the raw materials that were utilized were FeCl₃ and FeSO₄.7H₂O. In order to characterize the sample size and determine the thermal properties (maximum temperature T_{max}. in oC,

heating rate T/t in $^{\circ}\text{C} / \text{sec}$ and specific absorption rate SAR in W/g , different suspensions of Fe_2O_3 MNPs were made (S1, S5, S10, S15, and S20) by adding 1 ml of distil water (DW) to X mg of Fe_2O_3 . These suspensions were then characterized using transmission electron Then, the 1000W ZVS low voltage induction heating board that was operated at low frequencies 100 kHz module fly back driver heater DIY Fig.1 and the thermometer digital infrared (IR) noncontact forehead colorful LCD gun laser IR body Fig.2 were used in this research to study the thermal properties of the sample. Fig.1: The 1000W ZVS low voltage induction heating board that was operated at low frequencies 100 kHz. Fig.2: The thermometer digital infrared [31, 32, 33, 34].

5. Results and discussion

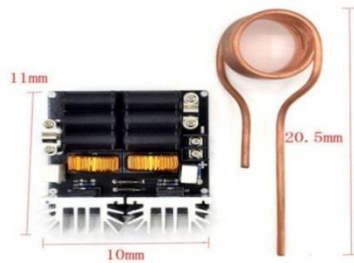


Fig.1: 1000W ZVS Low Voltage Induction Heating Board Module Fly Back Driver Heater DIY



Fig.2: Thermometer Digital Infrared Noncontact Forehead Colorful LCD Gun Laser IR body

After substituting the data of three of the sample's strongest peaks into the Scherer's Equation, we used an image from a Transmission Electron Microscope (TEM) and X-Ray Diffraction (XRD) patterns of the Fe_2O_3 MNPs (shown in Figures 3 and 4) to determine the sample's size. These figures can be found in Figures 3 and 4.1

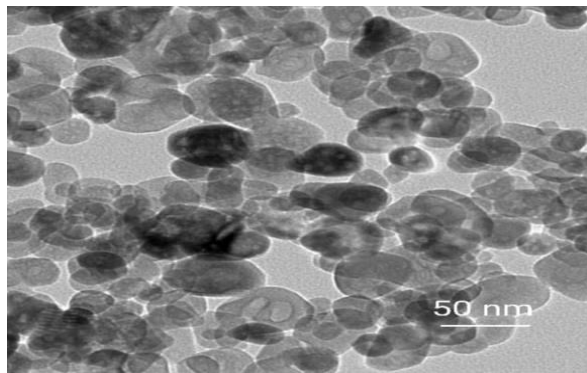


Fig.3: TEM image of Fe_2O_3 MNPs

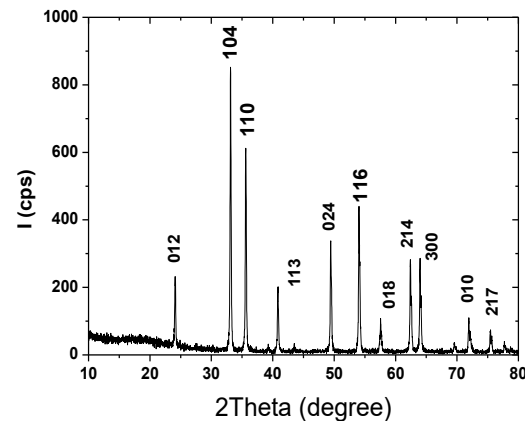


Fig.4: XRD pattern of Fe_2O_3 MNPs

$$t = \frac{K\lambda}{B \cos \theta} \quad (1)$$

Where; the thickness of the sample is (t), K is constant equal 0.9, the wavelength of Cu target in the XRD is $\lambda = 1.4506 \text{ \AA}$, the full width at half maximum (FWHM) is (B) and the Bragg's angle is (θ). The results of the average size conformal by TEM ($t = 38 \text{ nm}$) and XRD ($t = 50 \text{ nm}$) explain the sample size in nanostructures, this result qualifies for many uses, whether in various industries or medical fields [35,36,37].

To determine the specific absorption rate (SAR) value the following equation has been used:

$$SAR = C_w \frac{\Delta T}{\Delta t} \frac{1}{m_{ferrite}} \quad (2)$$

Where; $C_w = 4.185 \text{ J g}^{-1} \text{ K}^{-1}$ is the specific heat capacity of water, $\Delta T/\Delta t$ in $^{\circ}\text{C}/\text{sec}$ the heating rate, $m_{ferrite} = X \text{ mg}$ of Fe_3O_4 MNPs. The results of the thermal properties of the sample are listed in Table 1.

Table 1: Fe₂O₃ MNPs thermal properties.

X (mg/ml)	C_w (J/ g. $^{\circ}\text{C}$)	The thermal properties results		
		$T_{\max.}$ ($^{\circ}\text{C}$)	$\Delta T/\Delta t$ ($^{\circ}\text{C}/\text{sec}$)	SAR(W/g)
1	4.185	50	28.3×10^{-3}	118.4
5		49	26.7×10^{-3}	22.4
10		46	25.0×10^{-3}	10.5
15		45	23.3×10^{-3}	6.5
20		42	18.3×10^{-3}	3.8

It is common knowledge that exposing a magnetic sample to external magnetic fields causes the sample to become capable of producing heat in accordance with the Néel and/or Brownian relaxation models. This heat that is generated is dependent on a number of parameters, including those that are associated with the magnetic field that is present in the environment, such as its intensity, frequency, and power. And anything else that is associated with the magnetic sample, such as the kind of sample, its dimensions, as well as its magnetic and thermal properties [38].

In order to study the thermal properties (maximum temperature $T_{\max.}$, heating rate T/t and specific absorption rate SAR) of a sample of Fe_2O_3 MNPs as a function of the concentration of the sample, 5 samples (S1, S5, S10, S15 and S20) were prepared with different concentrations (1, 5, 10, 15, and 20 mg of Fe_2O_3 MNPs / ml of DW) respectively. These samples were then compared to one another After that, suspensions of Fe_2O_3 MNPs were generated using the different concentrations listed above (S1, S5, S10, S15, and S20), and each sample was subjected to an external magnetic field with a low frequency of 100 kilohertz while the circumstances remained the same. We found that: the temperature rises with the passage of time, and the maximum value $T_{\max.} = 50, 49, 46, 45,$ and $42 \text{ }^{\circ}\text{C}$ is reached after 30 minutes, where it remains for up to 60 minutes' total. This is recorded in Fig.5 and occurs because the heat that is produced as a result of the electromagnetic energy that is absorbed by Fe_2O_3 MNPs then releases it into the surroundings.

The results of the thermal properties for the samples (S1, S5, S10, S15, and S20) of different concentrations (1, 5, 10, 15, and 20) mg of Fe₂O₃ MNPs / 1ml of DW are shown in Figure 6. These results show that: there are no differences affecting the results of the maximum temperature T_{max} . and the heating rate T/t , but there is a clear difference in the results of the specific absorption rate SAR. It is important to notice that the suspension S1 had the highest value ($X = 1$ mg Fe₂O₃ MNPs / 1 ml of DW), while the suspension S20 had the lowest value ($X = 20$ mg Fe₂O₃ MNPs / 1 ml of DW), which demonstrates the inverse proportion that exists between SAR and the concentration of Fe₂O₃ MNPs.

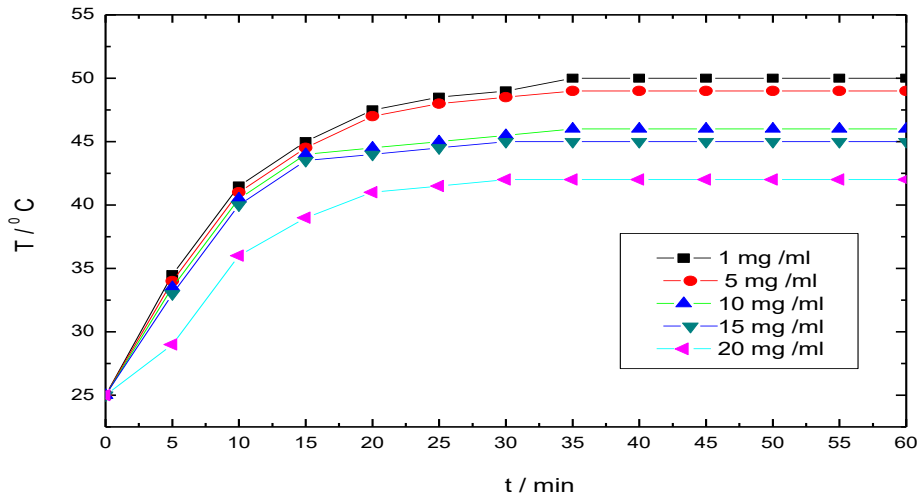


Fig.5: Fe₂O₃ MNPs heating rate.

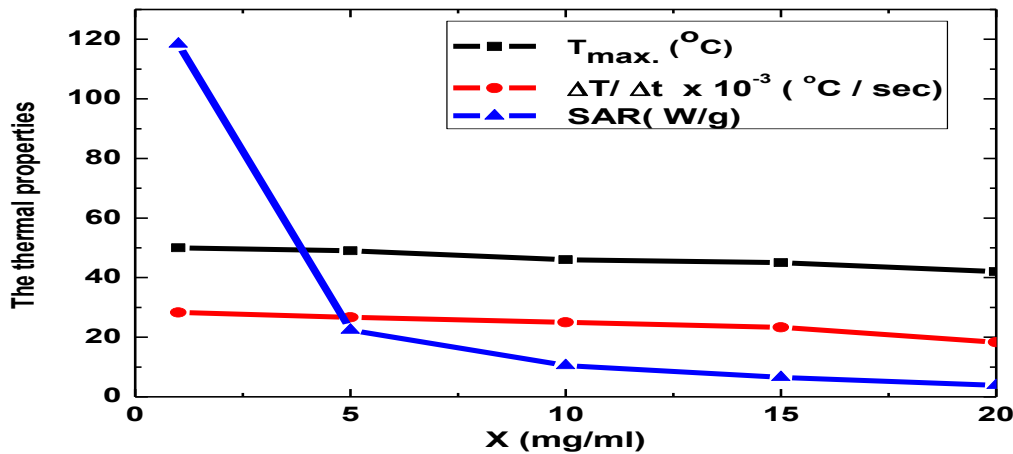


Fig.6: The thermal properties of Fe₂O₃ MNPs as a function of the concentration (X mg/ml)

6. Conclusion

The maximum temperature of Fe₂O₃ MNPs, measured in degrees Celsius (°C), the heating rate of Fe₂O₃ MNPs, measured in degrees Celsius (°C) per second, and the specific absorption rate of Fe₂O₃ MNPs, measured in watts

per gramme, all decrease as the concentration of Fe₂O₃ MNPs increases when the frequency is low. The maximum temperatures reached were 50, 49, 46, 45, and 42 degrees Celsius, and the amount of time required to reach each of these temperatures was 30 minutes. The concentrations of 1, 5, 10, 15, and 20 mg of Fe₂O₃ MNPs /ml were used in this experiment. These findings suggest that: a low concentration of the Fe₂O₃ MNPs should be used in order to achieve favorable outcomes for the substance's thermal properties.

7. Acknowledgements

The authors would like to express their gratitude to the departments of physics at Almahwah university, Albaha university, Dammam university, education college, and King Fahd university of petroleum and minerals for their contributions.

8. Data availability

The data that support the findings of this study are available from the corresponding author upon reasonable request.

9. References.

1. Sarafraz, M. M., Pourmehran, O., Yang, B., Arjomandi, M., & Ellahi, R. (2020). Pool boiling heat transfer characteristics of iron oxide nano-suspension under constant magnetic field. *International Journal of Thermal Sciences*, 147, 106131.
2. Aldaoud, A., Lemine, O. M., Ihzaz, N., El Mir, L., Alrub, S. A., & El-Boubbou, K. (2022). Magneto-thermal properties of Co-doped maghemite (γ -Fe₂O₃) nanoparticles for magnetic hyperthermia applications. *Physica B: Condensed Matter*, 639, 413993.
3. Hasan, S. G. A., AVSSKS, G., Reddi, B. V., & Sreeram Reddy, G. (2018). A critical review on preparation of Fe₃O₄ magnetic nano-particles and their potential application. *Int J Curr Eng Technol*, 8, 1613-1618.
4. Q. A. Pankhurst, J. Connolly, S. K. Jones & Dobson (2003), J. Applications of magnetic nano-particles in biomedicine. *Journal of Physics D: Applied Physics*, 36, R167–R181.
5. T.E. Torres, A.G. Roca, M.P. Morales, A. Ibarra, C. Marquina, M.R. Ibarra, and G.F. Goya (2009), *International Conference on Magnetism ICM*.
6. G F Goya, Jr. G F Lima, A D Arelaro, T Torres, H R Rechenberg, L Rossi, C Marquina and M R Ibarra (2008) *IEEE Trans. Magn. Magn.*, 44 4444.
7. J. Giustini Andrew, A. Peteryk Alicia, M. Cassim Shiraz, A. Tate Jennier and Ian Baker, P. Jack Hoops (2010), *Magnetic Nanoparticle Hyperthermia in Cancer Treatment*, Nano LIFE Vol. 1, Nos. 1 & 2 17_32 © World Scientific Publishing Company DOI: 10.1142/S1793984410000067.
8. David Aurélio, Jiří Mikšátko, Miroslav Veverka, Magdalena Michlová, Martin Kalbáček and Jana Vejpravová (2021) *Thermal Traits of MNPs under High-Frequency Magnetic Fields: Disentangling the Effect of Size and Coating*, *nanomaterials*, MDPI.
9. Y. Chen, M. Ruan, Y.F. Jiang, S.G. Cheng and W. Li, (2010) The synthesis and thermal effect of CoFe₂O₄ nanoparticles, *Journal of Alloys and Compounds*, journal homepage: www.elsevier.com/locate/jallcom.
10. Wu, S., & Ortiz, C. R. (2020). Experimental investigation of the effect of magnetic field on vapour absorption with LiBr–H₂O nanofluid. *Energy*, 193, 116640.
11. Mekonnen, T. W., Birhan, Y. S., Andrgie, A. T., Hanurry, E. Y., Darge, H. F., Chou, H. Y., ... & Chang, Y. H. (2019). Encapsulation of gadolinium ferrite nanoparticle in generation 4.5 poly (amidoamine) dendrimer for cancer theranostics applications using low frequency alternating magnetic field. *Colloids and Surfaces B: Biointerfaces*, 184, 110531.
12. Farahani, S. D., Alibeigi, M., & Farahani, H. H. (2021). The Uniform Magnetic Field Efficacy on Heat Transfer of Nanofluid Flow in A Flat Tube. *Journal of Advanced Research in Numerical Heat Transfer*, 5(1), 9-27.

13. Arya, H., Sarafraz, M. M., & Arjomandi, M. (2019). Pool boiling under the magnetic environment: experimental study on the role of magnetism in particulate fouling and bubbling of iron oxide/ethylene glycol nano-suspension. *Heat and Mass Transfer*, 55(1), 119-132.
14. Prabhakar, M. J., Jaisingh, J., & VR, A. P. (2020). Role of Magnetite (Fe₃O₄)-Titania (TiO₂) hybrid particle on mechanical, thermal and microwave attenuation behaviour of flexible natural rubber composite in X and Ku band frequencies. *Materials Research Express*, 7(1), 016106.
15. Hajahmed, M. (2019). Effect of Nano-particles on the Magnetic Field Induction for Iron Fillings Crushed for Different Crushing Times (Doctoral dissertation, Sudan University of Science and Technology).
16. Hajahmed, M. (2019). Effect of Nano-particles on the Magnetic Field Induction for Iron Fillings Crushed for Different Crushing Times (Doctoral dissertation, Sudan University of Science and Technology).
17. Kahali, P., Montazer, M., & Dolatabadi, M. K. (2022). Attachment of Tragacanth gum on polyester fabric through the synthesis of iron oxide gaining novel biological, physical, and thermal features. *International Journal of Biological Macromolecules*, 207, 193-204.
18. Bhandari, A. (2021). Water-based ferrofluid flow and heat transfer over a stretchable rotating disk under the influence of an alternating magnetic field. *Proceedings of the Institution of Mechanical Engineers, Part C: Journal of Mechanical Engineering Science*, 235(12), 2201-2214.
19. Merizgui, T., Hadjadj, A., Kious, M., Prakash, V. A., & Gaoui, B. (2019). Effect of magnetic iron (III) oxide particle addition with MWCNTs in kenaf fibre-reinforced epoxy composite shielding material in 'E', 'F', 'I' and 'J' band microwave frequencies. *Materials Research Express*, 6(4), 046102.
20. Flores-Rojas, G. G., López-Saucedo, F., Vera-Graziano, R., Mendizabal, E., & Bucio, E. (2022). Magnetic Nanoparticles for Medical Applications: Updated Review. *Macromol*, 2(3), 374-390.
21. Aldaoud, A., Lemine, O. M., Ihzaz, N., El Mir, L., Alrub, S. A., & El-Boubbou, K. (2022). Magneto-thermal properties of Co-doped maghemite (γ -Fe₂O₃) nanoparticles for magnetic hyperthermia applications. *Physica B: Condensed Matter*, 639, 413993.
22. Rajan, A., Sharma, M., & Sahu, N. K. (2020). Assessing magnetic and inductive thermal properties of various surfactants functionalised Fe₃O₄ nanoparticles for hyperthermia. *Scientific reports*, 10(1), 1-15.
23. Zysler, R. D., Fiorani, D., & Testa, A. M. (2001). Investigation of magnetic properties of interacting Fe₂O₃ nanoparticles. *Journal of magnetism and magnetic materials*, 224(1), 5-11.
24. Elbeshir, E. I. A. (2021). On the gum arabic to improve the thermal properties of Fe₃O₄ nanoparticles. *AIP Advances*, 11(4), 045224.
25. Soares, P. I., Lochte, F., Echeverria, C., Pereira, L. C., Coutinho, J. T., Ferreira, I. M., ... & Borges, J. P. (2015). Thermal and magnetic properties of iron oxide colloids: influence of surfactants. *Nanotechnology*, 26(42), 425704.
26. Rytov, R. A., Bautin, V. A., & Usov, N. A. (2022). Towards optimal thermal distribution in magnetic hyperthermia. *Scientific Reports*, 12(1), 1-9.
27. Ashjaee, M., Afgh, S. S. S., & Karimi, A. (2014). Experimental investigation on thermal conductivity of MFe₂O₄ (M= Fe and Co) magnetic nanofluids under influence of magnetic field.
28. Shylaja, A., Manikandan, S., Suganthi, K. S., & Rajan, K. S. (2015). Preparation and thermo-physical properties of Fe₂O₃-propylene glycol nanofluids. *Journal of Nanoscience and Nanotechnology*, 15(2), 1653-1659.
29. Lukawska, A. B. (2014). Thermal Properties of Magnetic Nanoparticles in External ac Magnetic Field.

30. Zouli, N., Mohammed, S. A. M., & Al-Dahhan, M. H. (2017). Enhancement of Heat Transfer Coefficient using Fe_2O_3 -Water Nanofluids.
31. Eltayeb I. A. Elbeshir, Abugomry (2016) Induction Heater Design to Study the Thermal Properties of Magnetic Nanoparticles, Journal of Physical Science and Application, doi: 10.17265/2159-5348/2016.04.007 Pa 51 -54.
32. Jun Motoyama, Toshiyuki Hakata, Ryuji Kato, Noriyuki Yamashita, Tomio Morino, Takeshi Kobayashi and Hiroyuki Honda(2008), Size dependent heat generation of magnetite nanoparticles under AC magnetic field for cancer therapy, Bio Magnetic Research and Technology, Bio Med Central.
33. Asahi Tomitaka, Minhong Jeun, Seongtae Bae, and Yasushi Takemura (2011), Evaluation of Magnetic and Thermal Properties of Ferrite Nanoparticles for Biomedical Applications, Journal of Magnetics 16(2), 164-168.
34. E. I. A. Elbeshir (2021), On the gum arabic to improve the thermal properties of Fe_3O_4 nanoparticles, AIP Advances 11(4):045224.
35. E. I. A. Elbeshir (2015), Synthesis and Specific Absorption Rate of Fe_3O_4 Nanoparticles, International Journal of Science and Research (IJSR) ISSN (Online): 2319-7064, Pa 932-934.
36. M.F. Nabil, W.H. Azmi, K.A. Hamid, N.N.M. Zawawi, G. Priyandoko and R. Mamat (2017), Thermo-physical properties of hybrid nanofluids and hybrid nanolubricants: A comprehensive review on performance, International Communications in Heat and Mass Transfer journal homepage: www.elsevier.com/locate/ichmt.
37. E. I. A. Elbeshir (2016), Evaluation of Thermal Properties of Ferrite Nanoparticles for Magnetic Hyperthermia Treatment, International Journal of Science and Research (IJSR) ISSN (Online): 2319-7064, Pa 291 – 294.
38. Jyotsnendu Giri, Pallab Pradhan, T. Sriharsha and D. Bahadur (2005), Preparation and investigation of potentiality of different soft ferrites, for hyperthermia applications JOURNAL OF APPLIED PHYSICS 97, 10Q916.